



# Preparation and properties of nano-hydroxyapatite/chitosan/carboxymethyl cellulose composite scaffold

Liuyun Jiang, Yubao Li\*, Xuejiang Wang, Li Zhang, Jiqui Wen, Mei Gong

Research Center for Nano-Biomaterials, Analytical and Testing Center, Sichuan University, Chengdu 610064, China

## ARTICLE INFO

### Article history:

Received 13 July 2007

Received in revised form 26 December 2007

Accepted 18 April 2008

Available online 1 May 2008

### Keywords:

Carboxymethyl cellulose

Nano-hydroxyapatite

Chitosan

Composite scaffold

Degradation

Bone tissue engineering

## ABSTRACT

Carboxymethyl cellulose was first incorporated into nano-hydroxyapatite/chitosan to obtain a novel composite of nano-hydroxyapatite/chitosan/carboxymethyl cellulose (n-HA/CS/CMC) as a three-dimensional scaffolds by freeze-drying. The surface morphology and properties of the scaffold were investigated by infrared absorption spectra (IR), X-ray diffraction (XRD), scanning electron microscope (SEM), mechanical testing and soaking in simulated body fluids (SBF) soaking. The results showed that strong chemical interactions were formed between the three phases. Moreover, the n-HA/CS/CMC composite scaffold with 30 wt% CMC had the most ideal porous structure with a pore size ranging from 100 to 500  $\mu\text{m}$  and a porosity 77.8%, and the highest compressive strength of 3.54 MPa. In addition, the SBF soaking experiment showed the scaffold of 30 wt% CMC had an acceptable degradation rate and good bioactivity *in vitro*. All the results suggest that n-HA/CS/CMC composite scaffolds have potential as bone tissue engineering materials.

© 2008 Elsevier Ltd. All rights reserved.

## 1. Introduction

Chitosan (CS), which is generally obtained by deacetylation of chitin, is a natural cationic polysaccharide. Due to its good biocompatibility and biodegradability, it has been widely used in the biomedical field (Park et al., 2000; Suh & Matthew, 2000), and it has been reported that it can promote adhesion and functional expression of osteoblasts because of its similarity to glycosaminoglycan in structure. Additionally, many researchers have shown that a material with a highly porous structure would provide more space for cells to attach and grow so that it has better biological properties (Lazzeri et al., 2006). So the CS sponge has been used for bone tissue engineering materials (Seol et al., 2004). To improve the bioactivity and mechanical properties so as to meet the basic requirement for rapid repair of bone, a promising method is to design a composite scaffold made of organic and inorganic phases according to the bionic approach (Li & Jiang, 2004). For the inorganic phase, nano-hydroxyapatite (n-HA) is an important candidate, because it can form a direct bond with bone due to its resemblance to bone mineral in chemical and crystal structure (Cook, Thomas, Dalton, Volkman, & Whitecloud, 1992; Noshi et al., 2000). There is thus considerable interest in developing n-HA/CS scaffold materials for bone tissue engineering. However, the n-HA/CS scaffold prepared by freeze-drying has a very poor compressive strength although it has better cell biocompatibility

than the CS scaffold *in vitro* (Kong et al., 2005). The scaffold made by the salt leaching method in our experiments has good compressive strength, but it has some cytotoxicity from the residue salt particles and a poor interconnected porous structure (Zhang et al., 2005b). To solve these problems, many researchers have added another organic polymer as a reinforcing phase, for example, gelatin, silk, etc. (Wang and Li, 2007; Zhao et al., 2002). However, the cost of developing a new material should also be taken into account. Carboxymethyl cellulose (CMC) obtained from natural cellulose by chemical modification is a water soluble cellulose ether derivate (Horner, Puls, Saake, Klotz, & Thielking, 1999), and is very similar to CS in structure. What is more important, it has opposite electric charge to CS, so CMC can react strongly with CS and act as an ionic cross-linking agent at the appropriate pH (Tiitu, Laine, Serimaa, & Ikkala, 2006). The composite of CMC/CS has been investigated by some researchers for possible medical applications on account of its excellent biocompatibility, biodegradability and hydrophilic surface (Hasan and Nurhan, 2004; Just & Majewicz, 1989). However, up to date, there is still no report on the preparation of a n-HA/CS/CMC composite scaffold. Therefore, here we first incorporated CMC into n-HA/CS to obtain a novel composite scaffold of n-HA/CS/CMC by freeze-drying to partly substitute CS with CMC.

In this paper, we describe the preparation of three n-HA/CS/CMC composite scaffolds with weight percentage of CMC of 40, 30 and 15 wt%. Properties including the porous structure, porosity, compressive strength, degradation rate and bioactivity *in vitro* were investigated.

\* Corresponding author. Tel./fax: +86 28 85417273.

E-mail address: [nic7504@scu.edu.cn](mailto:nic7504@scu.edu.cn) (Y. Li).

## 2. Experimental

### 2.1. Materials and methods

CS powder (degree of deacetylation 80%, viscosity molecular weight of  $2.5 \times 10^5$ ) was purchased from Haidebei Bioengineering Co., Ltd, Jinan, China. n-HA was prepared according to the previous report (Wang, Li, Wei, & Klass, 2002). CMC-Na (substitution degree of 0.7, viscosity molecular weight of about  $4.2 \times 10^8$ ) was purchased from Kelong Chemical Agent Factory, Chengdu, China. Other reagents used in this experiment were all of analytical grade.

### 2.2. Preparation of n-HA/CS/CMC composite scaffold

The n-HA/CS/CMC scaffolds were fabricated by the following procedure, and the original amount of the three components used here were listed in Table 1. CS and CMC powders were mixed and then added into a n-HA slurry (the water content is 98 wt%) with constant stirring. Afterward, the mixture was kept stirring for 2 h under ambient condition until the powders were thoroughly dispersed in the slurry, followed by the addition of a suitable amount of acetic acid (2 wt% acetic acid in the mixture), and the stirring was continued until the mixture solidified. Then the mixture was frozen at  $-30^\circ\text{C}$  for 12 h. Finally, the sample was transferred into a freeze-drying vessel for at least 30 h to get a porous scaffold. The scaffold was immersed in 10% NaOH solution for 2 h to neutralize the residue acetic acid, washed with deionized water and dried in a vacuum oven at  $60^\circ\text{C}$ .

### 2.3. Properties of n-HA/CS/CMC composite scaffold

The interactions of the three components were determined by IR (Spectrum 200, Perkin-Elmer) using the KBr disc technique and XRD using X'pert Pro MPD (Philip, The Netherlands) at a voltage and current of 40 kV and 30 mA.

The porous morphology of the scaffold was examined with SEM (JSM-5900LV, Japan). The scaffold sample was coated with gold, and the examination was carried out at an accelerating voltage of 20 kV.

The porosity was determined by the liquid displacement method (Zhang & Zhang, 2001). The procedure was as follows: First, the volume and weight of the sample were measured, noted as  $V_0$  and  $W_0$ , respectively. Secondly, the sample was immersed into the dehydrated alcohol for 48 h until it was saturated by absorbing dehydrated alcohol, and the sample was weighed again and noted as  $W_1$ . Finally, the porosity of the sample was calculated based on the formula of  $P = (W_1 - W_0)/(\rho V_0)$ , where  $\rho$  represents the density of dehydrated alcohol. Three parallel samples were carried out for every scaffold and the mean value of the porosities of different scaffolds were given.

The compressive strength was tested with a universal material testing machine (AG-10AT, Japan) with a compression strain rate of  $5 \text{ mm min}^{-1}$  until 50% reduction in specimen height. The scaffold sample was cut into cylindrical blocks with a size of  $\Phi 6 \times 12 \text{ mm}$ . Five parallel samples were tested for every scaffold and the mean value of the compressive strength of different scaffolds were given.

**Table 1**

The original amount of three component for the preparation of n-HA/CS/CMC composite scaffolds

n-HA/CS/CMC (CMC wt%)	n-HA (g)	CS (g)	CMC (g)
40	2	4	4
30	4	3	3
15	7	1.5	1.5

The *in vitro* degradation and bioactivity of the n-HA/CS/CMC composite scaffolds were investigated by SBF soaking for different period. The SBF solution was prepared by dissolving reagent chemicals of NaCl (7.996 g),  $\text{NaHCO}_3$  (0.350 g), KCl (0.224 g),  $\text{K}_2\text{HPO}_4 \cdot 3\text{H}_2\text{O}$  (0.228 g),  $\text{MgCl}_2 \cdot 6\text{H}_2\text{O}$  (0.305 g),  $\text{CaCl}_2$  (0.278 g) and  $\text{Na}_2\text{SO}_4$  (0.071 g) into less than 1000 ml deionized water. The fluid was buffered at physiological pH 7.40 at  $37^\circ\text{C}$  with tri-(hydroxymethyl) aminomethane (6.057 g) and hydrochloric acid, and the solution was made up to 1000 ml with additional water (Kokubo, Kushitani, Sakka, Kitsugi, & Yamamuro, 1990). The ion concentrations of SBF here are very close to those of human blood plasma. The dried samples were weighed and immersed in a tube containing 10 ml of SBF solution, kept oscillating at  $37.0 \pm 0.5^\circ\text{C}$  water bath. After soaking for 1, 2, 3, 4, 6 and 8 weeks, the samples were withdrawn from SBF, respectively, gently rinsed with deionized water and weighed again after being dried. The rate of weight loss ( $W_L$ ) was calculated according to the formula of  $W_L = (W_0 - W_1)/W_0 \times 100\%$ , where  $W_0$  and  $W_1$  denote the weight of the sample before and after soaking, respectively. Similarly, three parallel samples were carried out for the scaffold and the mean value of the rate of weight loss after soaking different periods were given. The sample with a 30 wt% CMC was selected as a representative sample for further bioactivity study, and the surface microstructure of the sample was observed by SEM after soaking for 4 and 8 weeks.

## 3. Results and discussion

### 3.1. IR analysis

In order to elucidate chemical interaction between the three phases, IR spectroscopy measurements were taken (Fig. 1). Comparing the IR spectra of pure n-HA, CS, CMC and n-HA/CS/CMC composite scaffolds, it can be found that the specific peaks of pure n-HA, CMC and CS all appear in the spectra of n-HA/CS/CMC composite scaffolds except for slight band-shifts as shown in Fig. 1c, d and e, which shows there is no change of the three compositions after preparation. However, an absorption at  $1655 \text{ cm}^{-1}$  in CS shifts

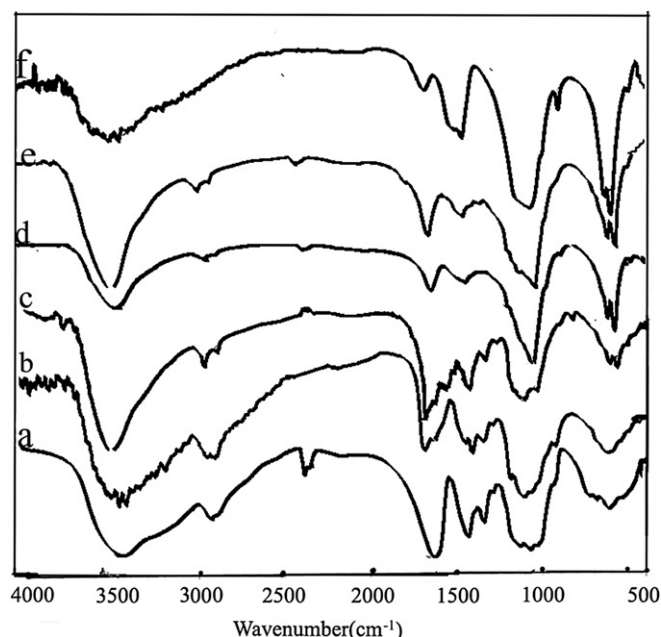


**Fig. 1.** IR spectra of (a) pure CMC, (b) pure CS, (c) 40 wt% CMC, (d) 30 wt% CMC, (e) 15 wt% CMC, (f) pure n-HA.

a little to low wavelengths in the three n-HA/CS/CMC composite scaffolds, which may be the result of the formation of  $\text{NH}_3^+$ . Additionally, the peak of asymmetry stretching of  $\text{COO}^-$  is still found at  $\sim 1420\text{ cm}^{-1}$ . Clearly, these observations mean that the strong electrostatic attraction between  $[\text{NH}_3^+]$  of CS and  $[\text{COO}^-]$  of CMC may be the main ion cross-linking interaction leading to the formation of polyelectrolyte network structure. At the same time,  $-\text{OH}$  has slight band-shifts in composite scaffolds, which suggests that there are some inter- or intra-hydrogen bonds among the three components of n-HA/CS/CMC composite scaffolds.

### 3.2. XRD analysis

Fig. 2 shows the X-ray diffraction patterns of pure n-HA, CS, CMC and n-HA/CS/CMC composite scaffolds. In Fig. 2a, two main diffraction peaks of CS at  $2\theta = 10^\circ$  and  $20^\circ$  are observed. In Fig. 2b, two main diffraction peaks of CMC at  $2\theta = 32^\circ$  and  $46^\circ$  can be found. The characteristic peaks of n-HA are shown in Fig. 2f. The XRD patterns of the n-HA/CS/CMC composite scaffolds shown in Fig. 2c, d and e are characterized by specific diffraction peaks arising from n-HA and CMC. However, the specific peaks for CS ( $2\theta = 20^\circ$ ) disappeared in the three composite scaffolds, which may be the result of the interaction of CS and CMC (Dong et al., 2004).

### 3.3. Structure of n-HA/CS/CMC composite scaffolds

The SEM images (Fig. 3) showed that the three scaffolds all have three-dimensional complicated irregular porous structures together with good interconnections between the pores (Fig. 3d and e), and the walls of the macropores contained many micropores (Fig. 3f). The pore size ranged from 100 to  $500\text{ }\mu\text{m}$ . In addition, the porosities all exceeded 70% (Fig. 4), which was determined with a liquid displacement method using dehydrated ethanol as the displacing liquid. Comparing the three scaffolds, it can be seen that the porosity of the scaffold became lower when the CMC content decreased. The reason may be that the CMC content decreased, and the higher percentage of n-HA occupied more space of ice in

the frozen mixture resulting in the lower porosity. In addition, among the three scaffolds, the 30 wt% CMC scaffold had the best ideal porous structure with the majority of macropore of the size  $400\text{ }\mu\text{m}$  or so, which may be helpful to promote cell adhesion and attachment, and conducive to tissue in-growth and nutrient delivery to the site of tissue regeneration (De Oliverira, De Aguiar, Rossi, & Soares, 2003; Wintermantel et al., 1996). Additionally, its porosity can also meet the requirement for bone tissue engineering scaffold materials.

### 3.4. Compressive strength of n-HA/CS/CMC composite scaffolds

For bone tissue engineering scaffold materials, the initial mechanical properties are usually an important criteria in selecting the scaffold materials. Here, the compressive strength of the three scaffolds were given (Fig. 5). From the data, it could be found that the compressive strength of the scaffold had a relation to the composition content, not only to the porosity. The reason may be that the too much n-HA could reduce the extent of ion cross-linking so that the polyelectrolyte network structure matrix may be insufficient to bind the higher percentage n-HA particles, resulting in poor mechanical properties. However, the compressive strength of 30 wt% CMC scaffold was the most satisfactory (3.54 MPa) when compared with that of bone (2–10 MPa) (Hutmacher, 2000). It means that the scaffold can support new bone tissue regeneration at the site of implantation and maintain sufficient integrity for both *in vitro* and *in vivo* cells (Chu, Orton, Hollister, Feinberg, & Halloran, 2002).

### 3.5. *In vitro* degradation test of n-HA/CS/CMC composite scaffold

Scaffold should have the advantage of degrading naturally over time as new tissue grows, so that it eliminates the need for further surgery. To further research the feasibility as bone tissue engineering scaffold materials, *in vitro* degradation of the n-HA/CS/CMC composite scaffolds were investigated. In this study, CMC, another degradable polymer, was added into the n-HA/CS system. Fig. 6 gives the rates of weight loss of the n-HA/CS/CMC scaffolds with different CMC contents as a function of soaking time in SBF. The rate of weight loss of the scaffolds increased up to 3 weeks and then decreased. The reason may be that the weight loss mainly results from the degradation of the scaffold and new apatite particles depositing on the scaffold. Up to the first 3 weeks, the degradation rate of the scaffold is predominantly of the scaffold is predominantly due to a decrease in the CS/CMC weight ratio. Then the weight loss rate decreased because more new apatite particles deposit. Among the three scaffolds, it can be seen that the scaffold with a 40 wt% CMC had a highest weight loss rate owing to the highest porosity and degradable composition as well as the lowest new apatite particles deposition rate. Similarly, the scaffold (15 wt% CMC) had the highest weight loss at the first week, which may be that more n-HA particles dissolved from the composite scaffold, then it had a similar weight loss tendency with that of the other two scaffolds expect for a lower weight loss.

In a word, the weight loss tendency of the n-HA/CS/CMC scaffolds is similar to that of n-HA/CS composite (Zhang et al., 2005a), which is regarded as degradable. Moreover, it can be inferred that the degradation rate of the n-HA/CS/CMC scaffold with a 30 wt% CMC may also be acceptable for bone tissue engineering scaffold materials if it was implanted in body on the condition of some enzymolysis (Hong et al., 2007; Muzzarelli et al., 2002).

### 3.6. The bioactivity of n-HA/CS/CMC composite scaffold *in vitro*

On the other hand, bone tissue engineering scaffold materials must exhibit high bioactivity to be used as an implant in body

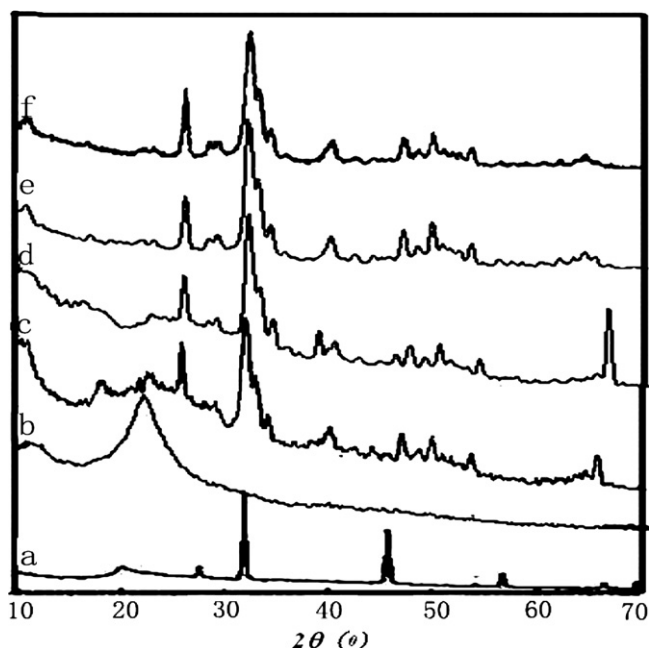


Fig. 2. XRD patterns of (a) pure CMC, (b) pure CS, (c) 40 wt% CMC, (d) 30 wt% CMC, (e) 15 wt% CMC, (f) pure n-HA.



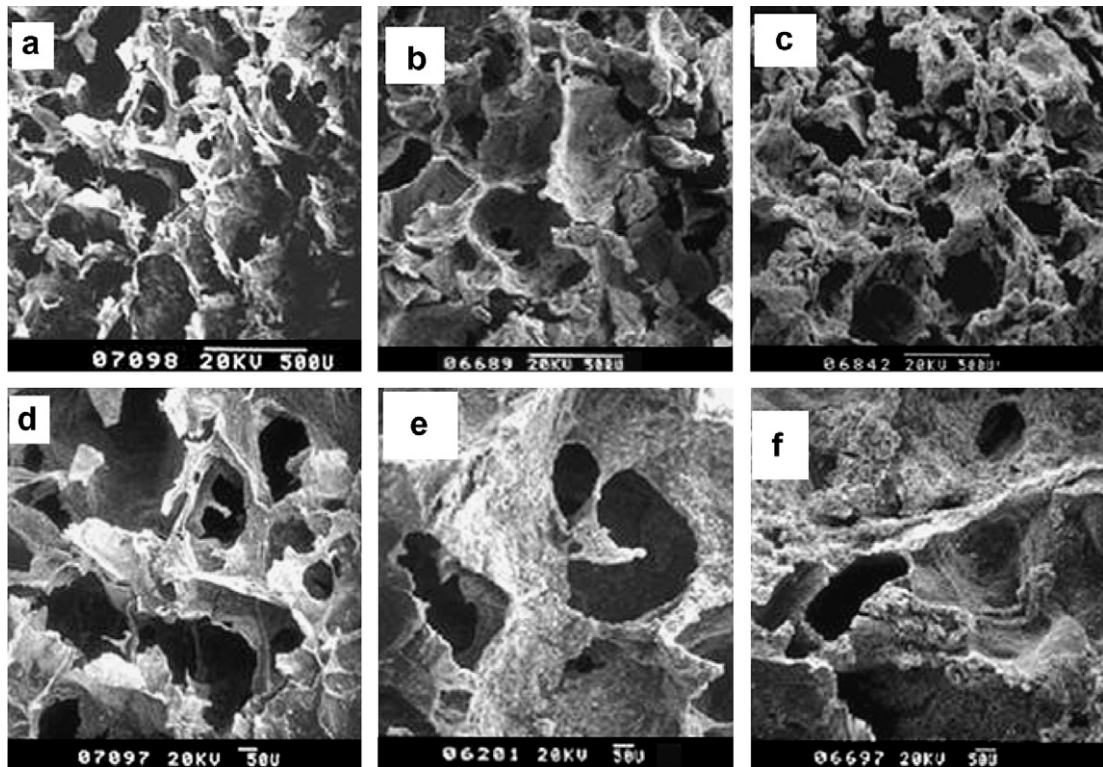


Fig. 3. SEM images of n-HA/CS/CMC composite scaffolds with different CMC content (a) and (d) for 40 wt%, (b) and (e) for 30 wt%, (c) and (f) for 15 wt%.

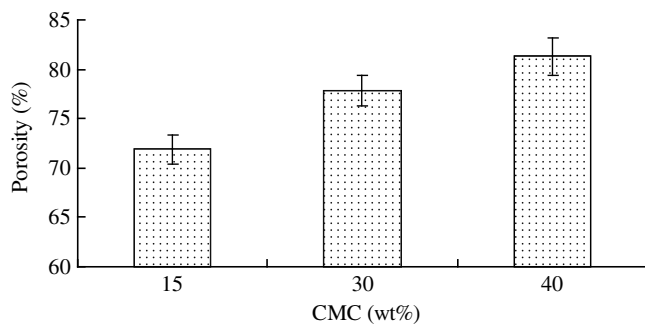


Fig. 4. The porosity of the n-HA/CS/CMC composite scaffolds as a function of CMC content (wt%).

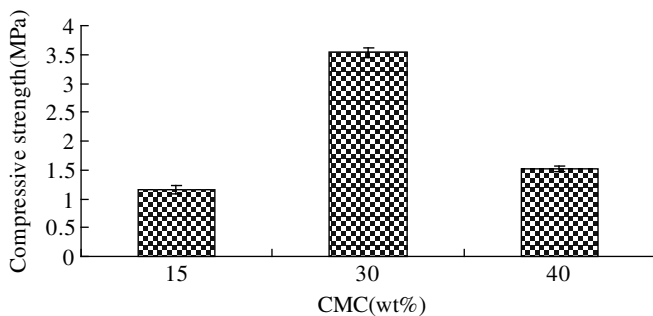


Fig. 5. The compressive strength of the n-HA/CS/CMC composite scaffold as a function of CMC content (wt%).

applications. In this study, *in vitro* bioactivity of the composite scaffold could be deduced from SEM microphotograph of the sample soaked in SBF. Fig. 7 shows the SEM microstructures of the n-

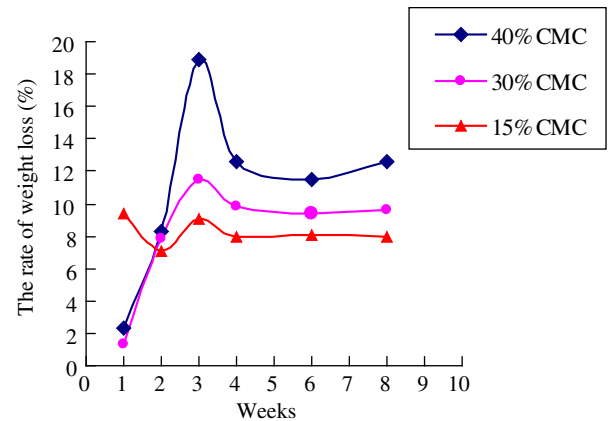


Fig. 6. The rate of weight loss of the n-HA/CS/CMC composite scaffolds as a function of soaking time.

HA/CS/CMC scaffold with 30 wt% CMC after soaking in SBF for 4 and 8 weeks, respectively. According to the SEM photos, it can be seen that some new apatite particles deposit on the surface from SBF solution after 4 weeks, as shown in Fig. 7a. After 8 weeks, more and more apatite particles were present on the surface and in the pores, and they aggregated to form an apatite layer, which can be seen in Fig. 7b. Based on the phenomenon of the apatite layer depositing on the scaffolds in SBF, it could be predicted that the scaffold can induce apatite particles to deposit in SBF and have good bioactivity *in vitro*, and it may have ability to make a direct bond to living bone when implanted in the body because of the resemblance of ion concentrations of SBF solution with that of blood plasma (Zhang et al., 2004).

Based on the above analyses, it can be concluded that the n-HA/CS/CMC composite scaffolds with a weight percentage of CMC of 30 wt% is the most ideal composite scaffold on account of its good

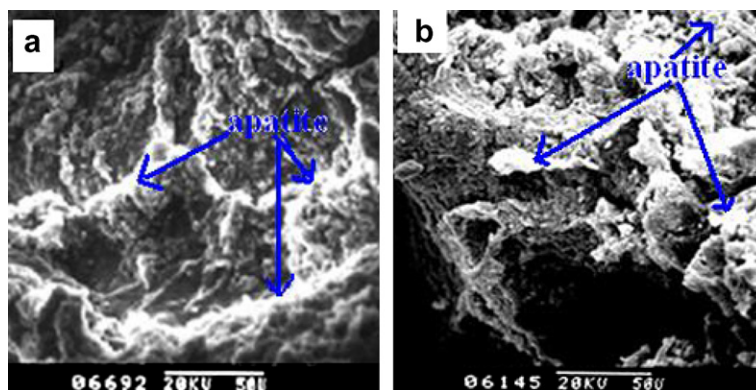


Fig. 7. SEM images of the n-HA/CS/CMC composite scaffold with CMC of 30 wt% after soaking in SBF (a) 4 weeks and (b) 8 weeks.

porous structure, high compressive strength, acceptable degradation rate and good bioactivity by SBF soaking experiment.

#### 4. Conclusions

In this study, we prepared n-HA/CS/CMC composite scaffolds by a simple and effective freeze-drying method without introducing any other poisonous cross-linking agents. The composite scaffold was formed by the main ion cross-linking interaction resulting from the  $[\text{NH}_3^+]$  of CS and  $[\text{COO}^-]$  of CMC, which is supported by IR and XRD analysis. Moreover, we can conclude that the novel n-HA/CS/CMC composite scaffold with CMC of 30 wt% is the most ideal scaffold with good three-dimensional complicated irregular porous structure, high compressive strength, acceptable degradation rate and good bioactivity, which provides a new approach to explore CMC of excellent biocompatibility, biodegradability and hydrophilic surface, a richer and cheaper natural polymer than CS, to be used for bone tissue engineering materials. As for the biological properties, the related research including *in vitro* cell culture and *in vivo* animal experiment are on going, and the corresponding results will be reported in next paper.

#### Acknowledgement

This work was funded by China–Netherlands programme strategic alliances (China 973 found: 2004CB720604).

#### References

- Chu, T. M., Orton, D. G., Hollister, S. J., Feinberg, S. E., & Halloran, J. W. (2002). Mechanical and *in vivo* performance of hydroxyapatite implants with controlled architectures. *Biomaterials*, 23, 1283–1293.
- Cook, S. D., Thomas, K. A., Dalton, J. E., Volkman, T. K., & Whitecloud, T. S. I. (1992). Hydroxylapatite coating of porous implants improves bone ingrowth and interface attachment strength. *Journal of Biomedical Materials Research*, 26, 989–1001.
- De Oliverira, J. F., De Aguiar, P. F., Rossi, A. M., & Soares, G. A. (2003). Effect of process parameters on the characteristics of porous calcium phosphate ceramics for bone tissue scaffolds. *International Social Artificial Organs*, 27, 406–411.
- Dong, Z. F., Du, Y. M., Fan, L. H., Wen, Y., Liu, H., & Wang, X. H. (2004). Preparation and properties of chitosan/gelatin/nano-TiO<sub>2</sub> ternary composite films. *Journal of Functional Polymers*, 17, 61–66.
- Hasan, T., & Nurhan, A. (2004). Carboxymethyl cellulose from sugar beet pulp cellulose as a hydrophilic polymer in coating of mandarin. *Journal of Food Engineering*, 62, 271–279.
- Hong, Y., Song, H. Q., Gong, Y. H., Mao, Z. W., Gao, C. Y., & Shen, J. C. (2007). Covalently cross-linked chitosan hydrogel: Properties of *in vitro* degradation and chondrocyte encapsulation. *Acta Biomaterialia*, 3, 23–31.
- Horner, S., Puls, J., Saake, B., Klotz, E. A., & Thielking, H. (1999). Enzyme-aided characterization of carboxymethyl cellulose. *Carbohydrate Polymers*, 40, 1–7.
- Hutmacher, D. W. (2000). Scaffolds in tissue engineering bone and cartilage. *Biomaterials*, 21, 2529–2943.
- Just, E. K., & Majewicz, T. G. (1989) (2nd ed.). *Encyclopedia of polymer science and technology* (Vol. 3). New York: Wiley. p. 226.
- Kokubo, T., Kushitani, H., Sakka, S., Kitsugi, T., & Yamamuro, T. (1990). Solution able to reproduce *in vivo* surface-structure changes in bioactive glass–ceramic A-W. *Journal of Biomedical Materials Research*, 24, 721–734.
- Kong, L. J., Gao, Y., Cao, W. L., Gong, Y. D., Zhao, N. M., & Zhang, X. F. (2005). Preparation and characterization of nano-hydroxyapatite/chitosan composite scaffolds. *Journal of Biomedical Materials Research*, 75A, 275–282.
- Lazzeri, L., Cascone, M. G., Serena, D., Serino, L. P., Moscato, S., & Bernardini, N. G. (2006). Gelatine/PLLA sponge-like scaffold: Morphological and biological characterization. *Journal of Materials Science: Materials in Medicine*, 17, 1211–1217.
- Li, Z., & Jiang, C. (2004). Preparation and characterization of macroporous chitosan/wollastonite composite scaffolds for tissue engineering. *Journal of Materials Science: Materials in Medicine*, 15, 625–629.
- Muzzarelli, R. A. A., Mattioli-Belmonte, M., Miliani, M., Muzzarelli, C., Gabbaneli, F., & Biagini, G. (2002). *In vivo* and *in vitro* biodegradation of oxchitin–chitosan and oxypullulan–chitosan complexes. *Carbohydrate Polymers*, 48, 15–21.
- Noshi, T., Yoshikawa, T., Ikeuchi, M., Dohi, Y., Ohgushi, H., & Horiuchi, K., et al. (2000). Enhancement of the *in vivo* osteogenic potential of marrow/hydroxyapatite composites by bovine bone morphogenetic protein. *Journal of Biomedical Materials Research*, 52, 621–630.
- Park, Y. J., Lee, Y. M., Park, S. N., Sheen, S. Y., Chung, C. D., & Lee, S. J. (2000). Platelet derived growth factor releasing chitosan sponge for periodontal bone regeneration. *Biomaterials*, 21, 153–159.
- Seol, Y. J., Lee, J. Y., Park, Y. J., Lee, Y. M., Ku, Y., Rhyu, I. C., et al. (2004). Chitosan sponges as tissue engineering scaffolds for bone formation. *Biotechnology Letters*, 26, 1037–1041.
- Suh, J. K., & Matthew, H. W. (2000). Application of chitosan-based polysaccharide biomaterials in cartilage tissue engineering: A review. *Biomaterials*, 21, 2589–2598.
- Tiitu, M., Laine, J., Serimaa, R., & Ikkala, O. (2006). Ionically self-assembled carboxymethyl cellulose/surfactant complexes for antistatic paper coatings. *Journal of Colloid and Interface Science*, 301, 92–97.
- Wang, L., & Li, C. Z. (2007). Preparation and physicochemical properties of a novel hydroxyapatite/chitosan–silk Wbroin composite. *Carbohydrate Polymers*, 68, 740–745.
- Wang, X. J., Li, Y. B., Wei, J., & de Groot, de GrootKlass (2002). Development of biomimetic nano-hydroxyapatite/poly (hexamethylene adipamide) composites. *Biomaterials*, 23, 4787–4791.
- Wintermantel, E., Mayer, J., Blum, J., Eckert, K. L., Lvscher, P., & Mathey, M. (1996). Tissue engineering scaffolds using superstructures. *Biomaterials*, 17, 83–91.
- Zhang, L. J., Feng, X. S., Liu, H. G., Qian, D. J., Zhang, L., & Yu, X. L., et al. (2004). Hydroxyapatite/collagen composite materials formation in simulated body fluid environment. *Materials Letters*, 58, 719–722.
- Zhang, L., Li, Y. B., Yang, A. P., Peng, X. L., Wang, X. J., & Zhang, X. (2005a). Preparation and *in vitro* investigation of chitosan/nano-hydroxyapatite composite used as bone substitute materials. *Journal of Materials Science: Materials in Medicine*, 16, 213–219.
- Zhang, L., Li, Y. B., Yang, A. P., Zuo, Y., Lv, G. Y., & Wei, J. (2005b). The preparation and characterization of porous scaffold made of nano-hydroxyapatite/chitosan composite for bone tissue engineering. *Functional Materials*, 36, 314–317.
- Zhang, Y., & Zhang, M. (2001). Synthesis and characterization of macroporous chitosan/calcium phosphate composite scaffolds for tissue engineering. *Journal of Biomedical Materials Research*, 55, 304–312.
- Zhao, F., Yin, Y. J., William, W., Lu, J., Leong, C. Y., & Zhang, W. Y., et al. (2002). Preparation and histological evaluation of biomimetic three-dimensional hydroxyapatite/chitosan–gelatin network composite scaffolds. *Biomaterials*, 23, 3227–3234.